Incorporation of Aqueous Reaction Kinetics and Biodegradation into TOUGHREACT: Application of a Multi-region Model to HydrobiogeoChemical Transport of Denitrification and Sulfate Reduction

Tianfu Xu

Earth Sciences Division
Lawrence Berkeley National Laboratory
One Cyclotron Road
Berkeley, CA 94720, USA

Abstract. The need to consider aqueous and sorption kinetics and microbiological processes arises in many subsurface problems. A general-rate expression has been implemented into the TOUGHREACT simulator, which considers multiple mechanisms (pathways) and includes multiple product, Monod, and inhibition terms. This paper presents a formulation for incorporating kinetic rates among primary species into mass-balance equations. The space discretization used is based on a flexible integral finite difference approach that uses irregular gridding to model bio-geologic structures. A general multi-region model for hydrological transport interacted with microbiological and geochemical processes is proposed. A 1-D reactive transport problem with kinetic biodegradation and sorption was used to test the enhanced simulator, which involves the processes that occur when a pulse of water containing NTA (nitrylotriacetate) and cobalt is injected into a column. The current simulation results agree very well with those obtained with other simulators. The applicability of this general multi-region model was validated by results from a published column experiment of denitrification and sulfate reduction. The matches with measured nitrate and sulfate concentrations were adjusted with the interficial area between mobile hydrological and immobile biological regions. Results suggest that TOUGHREACT can not only be a useful interpretative tool for biogeochemical experiments, but also can produce insight into processes and parameters of microscopic diffusion and their interplay with biogeochemical reactions. The geometric- and process-based multi-region model may provide a framework for understanding field-scale hydrobiogeochemical heterogeneities and upscaling parameters.

Key words: Aqueous reaction kinetics, Bacterial growth, TOUGHREACT, Multi-region model, Reactive Transport, Denitrification, Sulfate Reduction

1. Introduction

TOUGHREACT (Xu and Pruess, 2001; Xu et al., 2006) is a numerical simulation program for chemically reactive nonisothermal flows of multiphase fluids in porous and fractured media. This program written in Fortran 77 was developed by introducing reactive geochemical transport processes into the multiphase fluid- and heat-flow simulator TOUGH2 (Pruess et al., 1999). The program has been distributed to the public through the U.S. Department of Energy's Energy Science and Technology Software Center (email: estsc@adonis.osti.gov; WorldWideWeb: http://www.osti.gov/estsc/). Additional information is available on at http://www-esd.lbl.gov/TOUGHREACT/.

A variety of subsurface thermo-physical-chemical processes can be considered under a wide range of conditions of pressure, temperature, water saturation, ionic strength, pH and Eh. Interactions between mineral assemblages and fluids can occur under local equilibrium or kinetic rates. The gas phase can be chemically active. Precipitation and dissolution reactions can change formation porosity and permeability. The program can be applied to many geologic systems and environmental problems, including geothermal systems, diagenetic and weathering processes, subsurface waste disposal, acid mine drainage remediation, contaminant transport, and groundwater quality. The capabilities for reactive fluid flow and geochemical transport have been demonstrated in Spycher et al. (2003), Sonnenthal et al (2005), and Xu et al. (2006).

In natural systems, many redox reactions (such as sulfide oxidation) that take place homogeneously within the aqueous phase are slow to achieve equilibrium and therefore violate the local equilibrium assumption inherent in the current formulation of TOUGHREACT for aqueous species. Here, the formulation for adding aqueous reaction and bacterial growth kinetics into TOUGHREACT is first presented. The general multi-region model embodied in the code for hydrobiogeochemical transport is illustrated. Then, the application of multi-region model to reactive transport of denitrification and sulfate reduction is presented to demonstrate its applicability.

2. Formulation

Flow and transport in geologic media are based on space discretization by means of integral finite differences (IFD) (Narasimhan and Witherspoon, 1976). The IFD method provides a flexible discretization for geologic media that allows the use of irregular grids, which is well suited for simulation of flow, transport, fluid-microbial-rock interactions in multi-region heterogeneous and fractured rock systems (see Section 3 for details). For regular grids, IFD is equivalent to conventional finite differences. An implicit time-weighting scheme is used for the individual components of flow, transport, and kinetic biogeochemical reactions. TOUGHREACT uses a sequential iteration approach (SIA) similar to Yeh and Tripathi (1991) and Simunek and Suares (1994). The transport of chemical and microbial species is solved on a component-by-component basis. The system of mixed equilibrium-kinetic biogeochemical reaction equations is solved on a grid-block-by-grid-block basis by Newton-Raphson iteration. The governing equations for fluid and heat flow and geochemical transport are given in Xu and Pruess (2001). Here, (1) mass-balance equations for batch biogeochemical system and (2) the rate law used for aqueous reaction kinetics and biodegradation will be presented.

2.1. Mass balance for batch biogeochemical system

The TOUGHREACT formulation for an aqueous equilibrium system was presented in Xu and Pruess (2001), which is based on mass balance in terms of primary (basis) species. In contrast to aqueous equilibrium, species involved in kinetic reactions, such as redox couples, are independent and must be considered as primary species (Steefel and MacQuarrie, 1996). For example, for the reaction

$$HS^- + 2O_2(aq) = SO4^{2-} + H^+ \qquad (1)$$

under kinetic conditions, both HS^- and $SO4^{2-}$ must be placed in the primary species list (Steefel, 1997). Thus, all redox reactions making use of these species must be decoupled in the input of the thermodynamic database. Based on the previous formulation (Xu and

Pruess, 2001), we have added kinetic aqueous reactions with rate expressions discussed in the next section.

At time zero (initial), the total concentrations of primary species j (T_j^0) are assumed to be known, and are given by

$$T_j^0 = c_j^0 + \sum_{k=1}^{N_x} \nu_{kj} c_k^0 + \sum_{m=1}^{N_p} \nu_{mj} c_m^0 + \sum_{n=1}^{N_q} \nu_{nj} c_n^0 \qquad j = 1 \ldots N_C \tag{2}$$

where superscript 0 represents time zero; c are concentrations; subscripts j, k, m, and n are the indices of primary species, aqueous complexes, minerals at equilibrium, and minerals under kinetic constraints, respectively; N_c, N_x, N_p, and N_q are the number of corresponding species and minerals; ν_{kj}, ν_{mj}, and ν_{nj} are stoichiometric coefficients of the primary species in the aqueous complexes, equilibrium, and kinetic minerals, respectively.

After a time step Δt, the total concentration of primary species j (T_j) is given by

$$T_j = c_j + \sum_{k=1}^{N_x} \nu_{kj} c_k + \sum_{m=1}^{N_p} \nu_{mj} c_m + \sum_{n=1}^{N_q} \nu_{nj} \left(c_n^0 - r_n \Delta t \right) \qquad j = 1 \ldots N_C \tag{3}$$

where r_n is the kinetic rate of mineral dissolution (negative for precipitation, units used here are unit per kilogram of water per time), a general multi-mechanism rate law was used (Xu et al., 2006). T_j^0 and T_j are related through generation of j among primary species as follows

$$T_j - T_j^0 = \sum_{l=1}^{N_a} \nu_{lj} r_l \Delta t \qquad \mathrm{j} = 1, \ldots \mathrm{N_C} \tag{4}$$

where l is the aqueous kinetic reaction (including biodegradation) index, N_a is total number of kinetic reactions among primary species, and r_l is the kinetic rate which is in terms of generation of one mole of product species, such as SO_4^{2-} per unit time.

Therefore, for product species the stoichometric coefficients ν_{lj} are positive, for reactant species they are negative. For reaction (1), ν_{lj} for SO_4^{2-} and H^+ are 1; for HS^- it's –1, and for O_2(aq) it's –2.

By substituting Equations (2) and (3) into Equation (4), and denoting residual function as F_j^c (which is zero in the limit of convergence), we have

$$\begin{aligned} F_j^c = \quad & (c_j - c_j^0) && \text{basis species} \\ & + \sum_{k=1}^{N_x} \nu_{kj}(c_k - c_k^0) && \text{equilibrium aqueous complexes} \\ & + \sum_{m=1}^{N_p} \nu_{mj}(c_m - c_m^0) && \text{equilibrium minerals} \\ & - \sum_{n=1}^{N_q} \nu_{nj} r_n \Delta t && \text{kinetic minerals} \\ & - \sum_{l=1}^{N_a} \nu_{lj} r_l \Delta t && \text{kinetics among basis species} \\ = \quad & 0 && j = 1 \ldots N_C \end{aligned} \tag{5}$$

According to mass-action equations, concentrations of aqueous complexes c_k can be expressed as functions of concentrations of the primary species c_j. Kinetic rates r_n and r_l are functions of c_j. The expression of r_n is given in Xu et al. (2006), and r_l will be presented later. No explicit expressions relate equilibrium mineral concentrations c_m to c_j. Therefore, N_P additional mass-action equations (one per mineral) are needed. Details on solution of the nonlinear system of equations by the Newton-Raphson iterative method are given in Xu et al. (1999). Notice that gas dissolution/exsolution, cation exchange, and surface complexation are included in TOUGHREACT, but for simplicity the formulation is not shown here.

2.2. Rate expressions

By following the expression of Curtis (2003) and adding multiple mechanisms (or pathways), a general-rate law for reactions among primary species (including aqueous and sorption reaction kinetics and biodegradation) is used,

$$r_i = \sum_{s=1}^{Mech} \left[\begin{array}{ll} k_i & \text{rate constant} \\ \times \prod_{j=1}^{N_l} \left(\gamma_j^{\nu_{i,j}} C_j^{\nu_{i,j}} \right) & \text{product terms} \\ \times \prod_{k=1}^{N_m} \dfrac{C_{i,k}}{K_{Mi,k} + C_{i,k}} & \text{monod terms} \\ \times \prod_{p=1}^{N_p} \dfrac{I_{i,p} + C_{i,p}}{I_{i,p}} & \text{inhibition terms} \end{array} \right] \tag{6}$$

where r_i is the reaction rate of the ith reaction, *Mech* is the number of mechanisms or pathways and s is the mechanism counter, k_i is a rate constant, (often denoted $v_{\max}$, mximum specific growth constant for biodegradation), γ_j is the activity coefficient of species j, C_j is the concentration of species j (with biodegradation the product term is usually biomass concentration), $v_{i,j}$ is a stoichiometric coefficient, N_l is the number of reacting species in the forward rate term (called product terms), N_m is the number of Monod factors (Monod terms), $C_{i,k}$ is the concentration of the kth Monod species, $C_{i,p}$ is the concentration of the pth inhibiting species, $K_{Mi,k}$ is the kth monod half-saturation constant of the ith species, N_P is the number of inhibition factors (inhibition terms), and $I_{i,p}$ is the pth inhibition constant. Equation (6) accounts for multiple mechanisms and multiple products, Monod, and inhibition terms, which can cover many rate expressions (Examples of rate expression will be given in Sections 4 and 5).

Three major subroutines have been added for aqueous kinetic reactions. The first reads data related to define aqueous kinetic reactions and rate expressions. The second calculates kinetic rates based on updated concentrations of primary species. The third calculates derivatives of the rate with respect to concentrations of primary species using a numerical method. The advantage of numerical derivatives is that if one changes the rate

expressions, the derivative subroutine is not required to change. Sorption kinetics and biodegradation reactions are accommodated within the framework of the aqueous kinetics. Adsorbed and bacterial species are placed in the list of primary species. Adsorbed species must be specified not subject to hydrological transport. Bacterial species (biomass) can be specified either subject or not subject to transport.

3. Multi-region Model

In vadose zones and groundwater systems, most redox reactions are catalyzed by bacteria. Most of these bacteria are fixed on the solid phase within aquifers (Harvey et al., 1989; Zysset et al., 1994) or in river sediments (van Beelen and Fleuren Kemila, 1989). Formation around bacteria of micro-zones of polysaccharidic gels and other bacteria limits the dispersion of metabolites and nutrients (Martin, 1985). It may also protect microorganisms against desiccation or hagocytosis, toxins, etc. This conglomerate, consisting of the fully hydrated polymeric gel and bacteria, is called biofilm. Most bacteria grow within an immobile biofilm region residing on the solid surface. Growth of the biofilm is limited by microscopic diffusion processes for nutrient delivery.

To better describe reaction and transport in these hydrobiogeochemical systems, here we present a general three-region model (Figure 1) consisting of: (1) a mobile region (a fraction of the porosity) called Hydro-Region, (2) an biofilm immobile region called Bio-Region (another fraction of the porosity), and (3) a solid particle region where mineral dissolution/precipitation and surface reaction may occur, called Chem-Region. The concept was adopted from our previous method of "multiple interacting continua" (MINC) for resolving “global” flow and diffusion of chemicals in fractured rock and their interaction with the “local” exchange between fracture and matrix rock (Figure 2). This method was first developed by Pruess and Narasimhan (1985) for fluid and heat flow in fractured porous media. The extension of the MINC method to reactive geochemical transport is described by Xu and Pruess (2001). Similarly, a “shrinking core” model was proposed for sulfide mineral oxidation by Wunderly and others (1996). As the reaction between oxygen and sulfide minerals within the particles progresses the radius of the unreacted core will gradully decrease, while the thickness of the oxidized shell increases.

Thus, the oxygen flux from the outside of the particle surface to the unreacted core decreases with time.

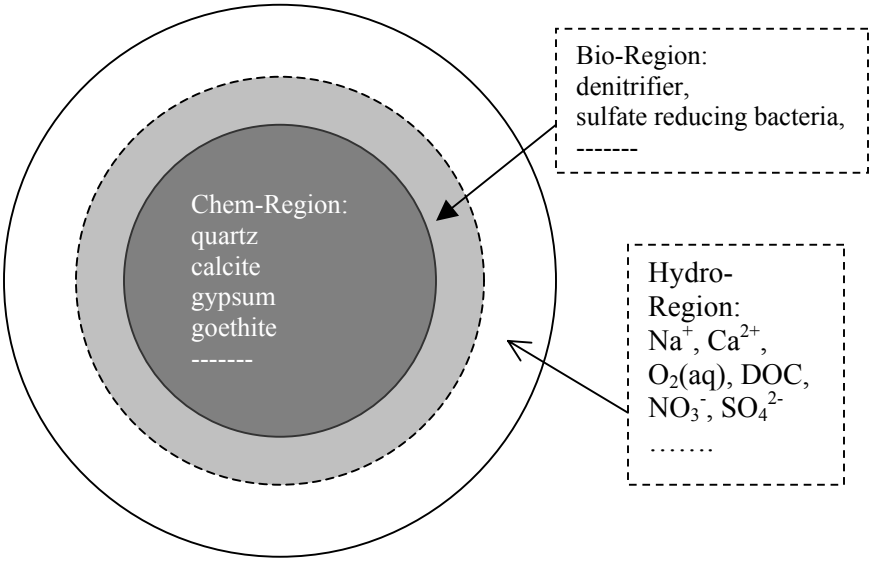

Figure 1. Concept of a Hydro-Bio-Chem Region model for resolving local diffusive transport.

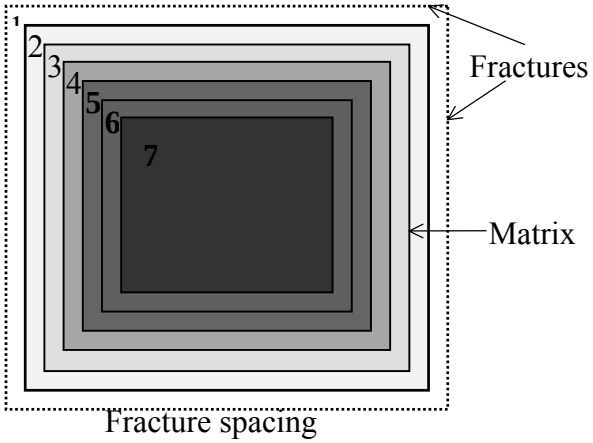

Figure 2. Subgridding of a rock matrix using "multiple interacting continua" (MINC) method.

In general, it is unnecessary to consider explicitly every pore and particle in a macro-grid block. All mobile portions of pores are lumped into Continuum # 1, Hydro-Region. All immobile biofilm portions of pores are lumped into Continuum # 2, Bio-Region. All particle volumes are lumped into Continuum # 3, Chem-Region. If necessary, each region can be further divided. For example, geochemical reactions often occur close to the particle surface, such that the portion close to the surface can be consided as one Chem-Region and the inner portion of the particle can be another Chem-Region. The regions are specified by means of a set of volume fractions VOL(j), j = 1, ..., J (where j is the region counter) into which the "primary" porous medium (macro-) grid blocks are partitioned. For microscopic diffusion processes, distances (d) and interfacial areas (A) between Hydro-Bio and Bio-Chem Regions are required to specify, or can be calibrated by matching observation data. The shapes, sizes and distributions of pores and particles are not required for the model.

Like TOUGH2, space discretization in TOUGHREACT is based on a flexible integral finite difference (IFD) approach. The IFD can deal with irregular grids, does not require reference to a global system of coordinates. TOUGHREACT can deal directly with classical dual-continua and multiple interacting continua fractured rocks as well as the Hydro-Bio-Chem-Region (HBCR) model for hydrobiogeochemical transport. The applicability of the HBCR to reactive transport of denitrification and sulfate reduction, and interplay between Bio- and Chem- Regions will be illustrated in Section 5.

4. Kinetic Biodegradation and Sorption

4.1. Problem setup

A biodegradation and sorption problem was used for testing TOUGHREACT against other simulators. A column of reactive biogeochemical transport originally developed by Tebes-Steven and Valocchi (1998) was employed. This problem was also used by others for verification of PHREEQC (Parkhurst and Appelo, 1999) and Bio-CORE2D (Zhang, 2001). This problem has several interacting chemical processes common to many environmental problems: biologically-mediated degradation of an organic substrate, bacterial cell growth and decay, metal sorption, and aqueous speciation

including metal-ligand complexation. The problem involves the transport processes when a pulse of water containing NTA (nitrylotriacetate) and cobalt is injected into a column. The problem includes advection and dispersion in the column, aqueous equilibrium reactions, and kinetic reactions for NTA degradation, growth of biomass, and cobalt sorption. The dimension and hydrological properties of the column are given in Table 1. Aqueous complexes considered and their stoichiometric coefficients and equilibrium constants are summarized in Table 2.

Table 1. Hydrological properties of the column.

Property	*Value*
Length of column	10 m
Porosity	0.4
Bulk density	1.5×10^3 kg/m^3
Grams of sediment per liter water (from porosity and bulk density)	3.75×10^3 g/l
Pore water velocity	1 m/hr
Longitudinal dispersivity	0.05 m

Table 2. List of stoichiometric coefficients and equilibrium constants for aqueous complexes.

Complex	*Stoichiometric coefficients*					*$Log_{10}K$*
	H^+	H_2CO_3	NH_4^+	NTA^{3-}	Co^{2+}	
H_3NTA	3			1		-14.9
H_2NTA^-	2			1		-13.3
$HNTA^{2-}$	1			1		-10.3
$CoNTA^-$				1	1	-11.7
$CoNTA_2^{4-}$				2	1	-14.5
$CoNTA^{2-}$	-1			1	1	-0.5
$CoOH^+$	-1				1	9.7
$Co(OH)_2$	-2				1	22.9
$Co(OH)_3^-$	-3				1	31.5
HCO_3^-	-1	1				6.35
CO_3^{2-}	-2	1				16.68
$NH_3(aq)$	-1		1			9.3
OH^-	-1					14.0

Table 3. List of concentrations for injection and background waters.

Component	*Mobile*	*Injection concentration (mol/l)*	*Initial concentration (mol/l)*
H^+	Yes	10×10^{-6}	10×10^{-6}
Total carbon	Yes	4.9×10^{-7}	4.9×10^{-7}
NH_4^+	Yes	0.0	0.0
O_2(aq)	Yes	3.125×10^{-5}	3.125×10^{-5}
NTA^{3-}	Yes	5.23×10^{-6}	
Co^{2+}	Yes	5.23×10^{-6}	
Na	Yes	1.0×10^{-3}	1.0×10^{-3}
Cl^-	Yes	1.0×10^{-3}	1.0×10^{-3}
Biomass	No	---	1.36×10^{-4}
CoNTA(ads)	No	---	0.0
Co(ads)	No	---	0.0

Biodegradation

The initial concentrations in the column are listed in Table 3. The column contains no NTA and cobalt initially, but has a biomass of 1.36×10^{-4} g/l. Injection water with NTA and cobalt is applied at the inlet of the column for 20 hours. Injection concentrations are also given in Table 3. After 20 hours, the background (initial) water is introduced at the inlet until the experiment ends (at 75 hours). NTA is assumed to degrade in the presence of biomass and oxygen according to the reaction:

$$HNta^{2-} + 1.62O_2(aq) + 1.272H_2O + 2.424H^+ = 0.576C_5H_7O_2N + 3.12H_2CO_3 + 0.424NH_4^+ \quad (7)$$

The NTA reaction converts 1 mol $HNTA^{2-}$ ($C_6H_7O_6N$) to 0.576 mol $C_5H_7O_2N$, where the latter is chemically inert, so that its concentration can be discarded. The following double Monod rate expression is used to describe the rate of NTA degradation:

$$r_{HNTA^{2-}} = k_{biom} X_{biom} \left(\frac{C_{HNTA^{2-}}}{K_s + C_{HNTA^{2-}}} \right) \left(\frac{C_{O_2}}{K_a + C_{O_2}} \right) \quad (8)$$

where $r_{HNTA^{2-}}$ is the rate of $HNTA^{2-}$ degradation (mol/l/hr), k_{biom} is the maximum specific rate of substrate utilization (mol/g cells/hr), X_{biom} is the biomass (g cells/l), K_s is the half-saturation constant for the substrate NTA (mol/l), K_a is the half-saturation constant for the electron acceptor O_2 (mol/l), and *C* donates concentration of species (mol/l). Rate expression (8), compared to the general form (6) has only one mechanism, one product term X_{biom}, and two Monod terms.

The rate of biomass production is dependent on the rate of substrate utilization and a first-order decay rate for the biomass:

$$r_{biom} = -yr_{HNTA^{2-}} - bX_{biom} \tag{9}$$

where r_m is the rate of cell growth (g cells/l/hr), *y* is the microbial yield coefficient (g cells/mol NTA), and *b* is the first-order biomass decay coefficient (hr^{-1}). The parameter values for Equations (8) and (9) are listed in Table 4. Rate expression (9) consists of two mechanisms using Equation (6).

Table 4. List of kinetic rate parameters used in Equations (8) and (9).

Parameter	*Description*	*Value*
K_s	half-saturation constant for donor	7.64×10^{-7} mol/l
K_a	half-saturation constant for acceptor	6.25×10^{-6} mol/l
k_{biom}	maximum specific rate of substrate utilization	1.418×10^{-3} mol/gcells/hr
y	microbial yield coefficient	65.14 g cells/mol NTA
b	first-order biomass decay coefficient	0.00208 hr^{-1}

Kinetic sorption

The rate expressions for kinetic sorption reactions involving Co^{2+} and $CoNTA^-$ are given by

$$r_i = -k_m\left(C_i - \frac{S_i}{K_d}\right) = -k_m C_i - \frac{k_m}{K_d} S_i \qquad (10)$$

where i is either Co^{2+} or $CoNTA^-$ (mol/L), S_i is the sorbed concentration (mol/g sediment), k_m is the mass-transfer coefficient (hr^{-1}), and K_d is the distribution coefficient (L/g). Values for the coefficients are given in Table 5. The values of K_d were defined to give retardation coefficients of 20 and 3 for Co^{2+} and $CoNTA^-$, respectively. Two mechanisms involved in the sorption kinetics are each represented by a product term, using Equation (6).

Table 5. Sorption coefficients for Co^{2+} and $CoNTA^-$.

Species	k_m	K_d
Co^{2+}	1 hr^{-1}	5.07×10^{-3} l/g
$CoNTA^-$	1 hr^{-1}	5.33×10^{-4} l/g

4.2. Comparison of results

The evolution of aqueous and immobile constituents at the outlet of the column is shown in Figure 3. In the experiment, two pore volumes of water with NTA and cobalt were introduced into the column over the first 20 hours, followed by 5.5 pore volumes of background water over the next 55 hours. At 10 hours, $HNta^{2-}$ begins to appear at the column outlet, along with a rise in the pH (Figure 3a). If NTA and cobalt were conservative and dispersion negligible, the graph would show square pulses that increase at 10 hours and decrease at 30 hours. However, the movement of the NTA and cobalt is retarded (relative to conservative movement) by the sorption reactions. The peak in NTA and cobalt concentrations occurs in the CoNta complex between 30 and 40 hours (Figures 3c and d), while the peak in Co^{2+} concentration is even more retarded by its sorption reaction and does not show up until near the end of the experiment. The sorbed $CoNta^-$ concentration peaks between 30 and 40 hours and slightly lags behind the peak in the dissolved concentration of the $CoNta^-$ complex. Initially, no NTA is present in the

column, and the biomass decreases slightly over the first 10 hours because of the first-order decay rate for the biomass (Figure 3b). As the NTA moves through the column, the biomass increases as the NTA substrate becomes available. After the peak of NTA has moved through the column, biomass concentrations level off and then begin to decrease because of decay. The *Kd* for cobalt sorption relates to a greater retardation coefficient than the *Kd* for $CoNta^-$ sorption, and the sorbed concentration of Co^{2+} appears to be still increasing at the end of the experiment. The TOUGHREACT simulation results agree well with those of Bio-CORE2D and PHREEQC, as well as with the original results given by Tebes-Steven and Valocchi (1998).

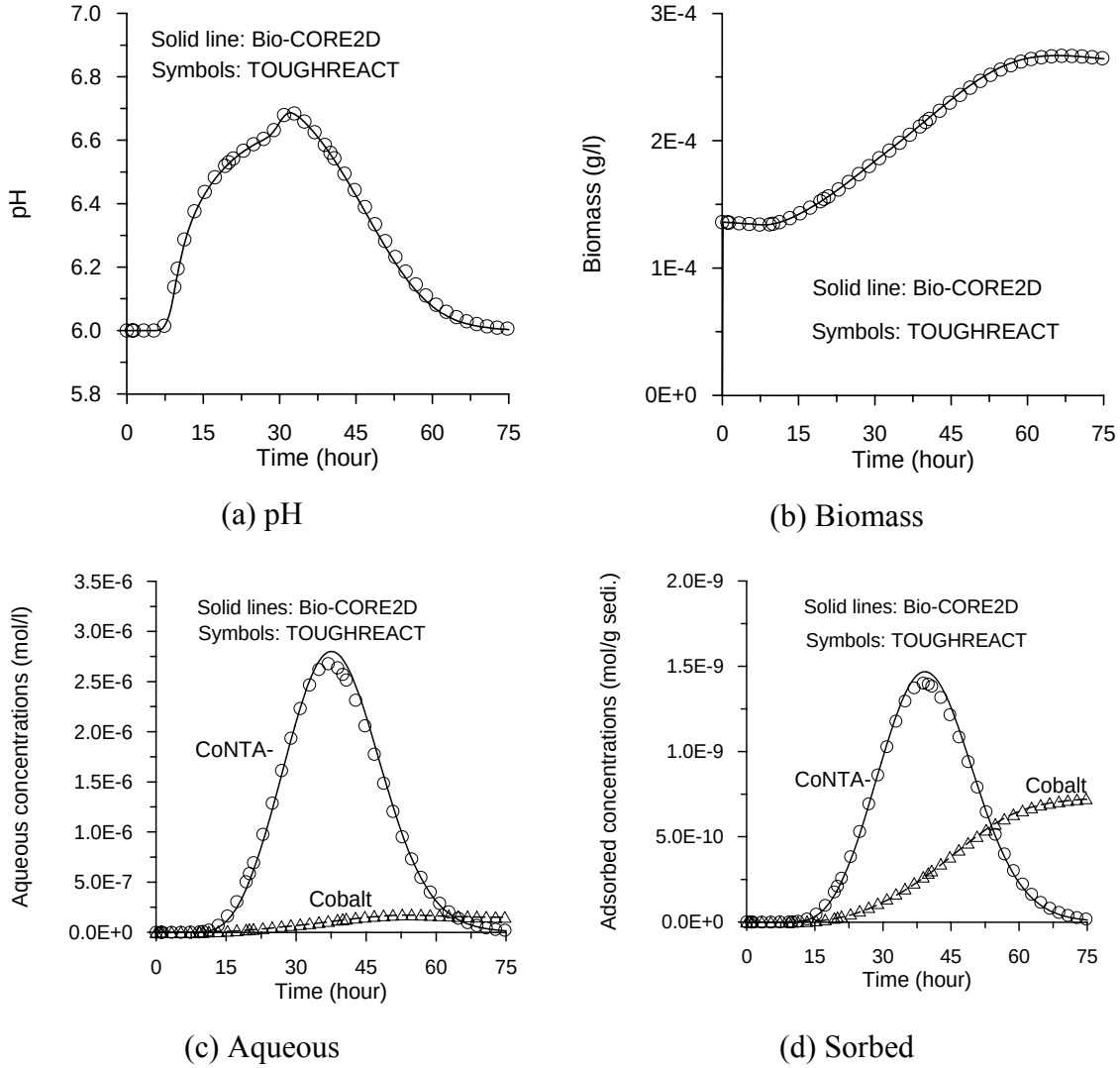

Figure 3. Simulation results for the 1-D biodegradation and sorption problem.

5. Denitrification and Sulfate Reduction

5.1. Problem statement

To test the applicability of the multi-region model embodied in TOUGHREACT for reactive transport of denitrification and sulfate reduction, the column experiments of von Gunten and Zobrist (1993) were modeled. The experimental data were first used by Zysset et al. (1994) for their macroscopic model involving the transport of dissolved substances in groundwater-biofilm systems. Zysset's model conceptualizes the diffusion-dominated microscopic transport processes within the biofilm by using a logistic approach based on a diffusional limitation. Biological processes were explicitly accounted for. Later, Doussan et al. (1997) used the same experimental data set for their model testing. They treated the diffusion dominated microscopic transport processes within the biofilm by using a mass-transfer coefficient in the macroscopic transport equations. These experiments were designed to simulate infiltration of an organically polluted river into an aquifer. Thus, synthetic river water, including an organic substrate (lactate) and electron acceptors of oxygen, nitrate and sulfate, were injected into columns filled with river sediments. In the first column, only nitrate is added to the solution as an electron acceptor. In the second column, oxygen, nitrate, and sulfate are used as electron acceptors.

5.2. Biodegradation kinetics and parameters

As described by the previous investigators, three major microbially-mediated reactions are involved in the experiments. Three electron acceptors are reduced, while dissolved organic matter (DOC) using lactate ($C_3H_5O_3^-$) in the experiment, are oxidized as follows:

$$3O_2(aq) + C_3H_5O_3^- \rightarrow 3HCO_3^- + 2H^+ - 2H_2O \quad (11)$$

$$12NO_3^- + 5C_3H_5O_3^- + 2H^+ \rightarrow 15HCO_3^- + 6N_2(aq) + 6H_2O \quad (12)$$

$$3SO_4^{2-} + 4C_3H_5O_3^- \rightarrow 4C_2H_3O_2^- + 4HCO_3^- + 3HS^- + H^+ \quad (13)$$

The bacterial growth rates due to three different electron acceptors are given in Equations (14), (15) and (16), respectively. Denitrification is inhibited by oxygen, and sulfate reduction is inhibited by both oxygen and nitrate. The rate parameters for Equations (14) through (16) are given in Table 6.

$$r_b^{O_2} = k_b^{O_2} X_b \left(\frac{C_{DOC}}{K_{DOC}^{O_2} + C_{DOC}} \right) \left(\frac{C_{O_2}}{K_{O_2} + C_{O_2}} \right) \tag{14}$$

$$r_b^{NO_3} = k_b^{NO_3} X_b \left(\frac{C_{DOC}}{K_{DOC}^{NO_3} + C_{DOC}} \right) \left(\frac{C_{NO_3}}{K_{NO_3} + C_{NO_3}} \right) \left(\frac{I_{O_2 \to NO_3}}{I_{O_2 \to NO_3} + C_{O_2}} \right) \tag{15}$$

$$r_b^{SO_4} = k_b^{SO_4} X_b \left(\frac{C_{DOC}}{K_{DOC}^{SO_4} + C_{DOC}} \right) \left(\frac{C_{SO_4}}{K_{SO_4} + C_{SO_4}} \right) \left(\frac{I_{O_2 \to SO_4}}{I_{O_2 \to SO_4} + C_{O_2}} \right) \left(\frac{I_{NO_3 \to SO_4}}{I_{NO_3 \to SO_4} + C_{NO_3}} \right) \tag{16}$$

The overall biomass growth rate is expressed as

$$r_b = r_b^{O_2} + r_b^{NO_3} + r_b^{SO_4} - bX_b \tag{17}$$

where X_b is biomass concentration (mg/l), b is decay constant, and a value of 5.787×10^{-7} 1/s was used according to Doussan et al. (1997). In this example, biomass is assumed not subject to transport. As mentioned in Section 3, most of the bacteria are fixed on the solid phase within geologic media. (It should be noticed that TOUGHREACT can handle transport of bacterial species.)

Table 6. List of biodegradation rate parameters used in Equations (14) through (16) (according to Doussan et al., 1997).

	O_2	NO_3	SO_4
Maximum specific growth constant k (1/s)	1.1574×10^{-4}	1.1667×10^{-5}	3.01×10^{-6}
Half-saturation constant of electron acceptors (mg/l)	0.77	7	5.35
Half-saturation constant of electron donor (mg/1)	3	3	3
Inhibition constants (mg/1)	$O_2 \to NO_3$ 10^{-3}		O_2 , $NO_3 \to SO_4$ 2×10^{-3}

5.3. **Denitrification**

In the first column, only nitrate is added to the solution as an electron acceptor. As mentioned above, Doussan et al. (1997) modeled the reactive transport of denitrification in Column 1. They treated the diffusion-dominated microscopic transport processes within the biofilm by a mass-transfer coefficient, which was calibrated by the experimental data. Maximum specific growth rates and half-saturation constants were also calibrated. These calibrated parameters were also used for their Column 2 simulation. In the present study, a porous medium model for the denitrification is first used. Then, the general multi-region model is applied for microscopic diffusive transport processes within the biofilm and solid particle.

Porous medium model

The porous 1-D flow system has a cross-sectional area of 1 m^2 (not the real area but a injection flow rate is specified at the inlet) and 0.1 m length, divided into 50 grid blocks of 0.002 spacing. The experiments were started by inoculating the water in the columns with a small amount of bacteria, but no biomass concentration is reported in von Gunten and Zobrist (1993). Here a starting biomass concentration of 0.15 mg/l, used by Zysset et al. (1994) for their model test, was employed. Initial concentrations for all other species are set equal to a very small value of 10^{-10} mg/l (practically zero, because TOUGHREACT uses log10 calculations for a better convergence). The boundary conditions used in the simulation are given in Table 7. A diffusion coefficient of 1×10^{-9} m^2/s was used. TOUGHREACT uses an upstream weighting scheme, resulting in a numerical dispersivity of $\alpha_n = \Delta x/2 = 0.001$ m, which equals the actual physical dispersivity used by Zysset et al. (1994).

The results of the porous medium model, together with the experimental data, are presented in Figure 4. The simulated curve after 7 days is slightly below the observed data. The 14-day curve is much lower than the data, indicating strong bio-reactions occurred within the porous model. In this model, bacteria are present throughout pore space (a 0.4 porosity). After the porous medium model was found unable to reproduce the experiment, the multi-region model as illustrated in Figure 1 was applied.

Table 7. Boundary conditions used in simulation of the column experiments.

	Column 1	Column 2
Injection flow rate (Darcy velocity, m/day)	1.8	0.37
O_2 (mg/l)		7
NO_3 (mg/l)	34.1	18.6
SO_4 (mg/l)		21.5
DOC (mg/l)	43.2	43.2

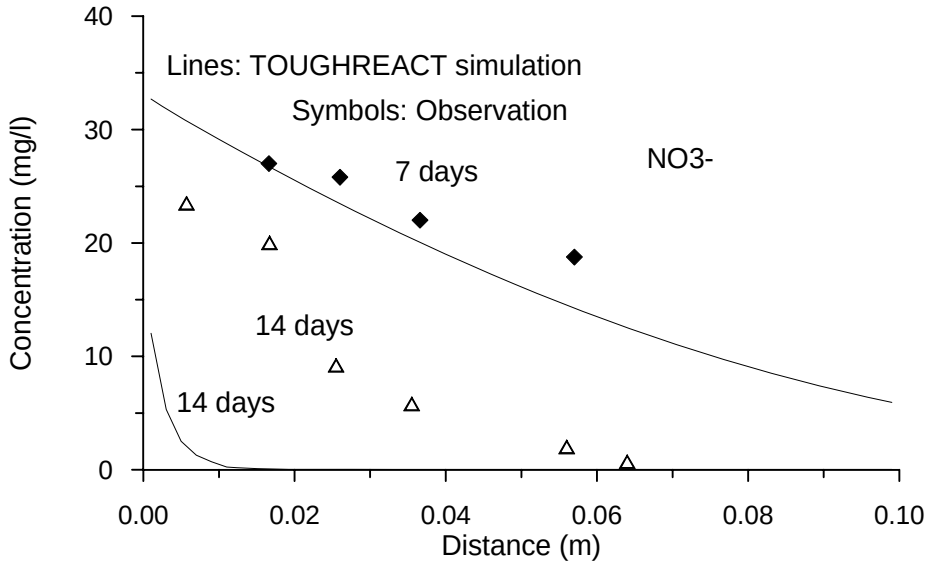

Figure 4. Simulated and observed nitrate concentrations along Column 1 after 7 and 14 days.

Multi-Region Model

The physical parameters used for the three regions are given in Table 8. For the first trial run, 15% of the bulk porosity (0.4) was assumed for the immobile Bio-Region. In the multi-region simulations, a porosity of 1 was assigned for both the Hydro- and the Bio- Region. Changes in porosity caused by bacterial growth are not currently considered. A 0.05 porosity was assumed for the Chem-Region. In Section 5.5, a mineral composition is assigned for the Chem-Region to illustrate the coupling of microbially-mediated redox reactions with mineral dissolution and precipitation. The distance (Table

8, $d = d_1 + d_2$) between the Hydro-Region and Bio-Region is assumed to be 2×10^{-5} m, a fraction of the sand particle sizes range from 1.252×10^{-4} to 2.52×10^{-4} m (von Gunten and Zobrist, 1993). The interficial area (A) was calibrated by matching the measured nitrate concentrations. The d between the Bio-Region and Chem-Region (3×10^{-5} m) was set slightly larger than the Hydro-, and Bio- Regions. The same A was used for Bio- and Chem- Regions. In fact, diffusive flux between regions is proportional to $D_0\tau A/d$, where D_0 is diffusion coefficient (10^{-9} m^2/s) and τ is tortuosity. The τ between two regions is calculated according to values in two regions (see Table 9) by $\tau = (d_1t_1+d_2t_2)/(d_1+d_2)$. Therefore, errors in d, D_0, and τ will be passed along to A. The other conditions and parameters are unchanged from the previous 1-D porous medium simulation.

Table 8. List of physical parameters used for the three regions.

Parameter	Hydro-Region		Bio-Region		Chem-Region	
Volume fraction of the medium	0.34		0.06 (15% of the bulk porosity)		0.60	
Porosity	1.0		1.0		0.05	
Distance (in m)		d_1	d_2	d_1	d_2	
		10^{-5}	10^{-5}	10^{-5}	2×10^{-5}	
Tortuosity	0.5		0.3		0.1	
		0.4		0.1667		

The concentration profile of nitrate at different times obtained with the multi-region model is presented in Figure 5. Starting from a 15% immobile region, the 7-day curve agrees well the observed data. However, the 14-day curve is above the corresponding data (less reactive), but improved from the porous model. This may result from bacterial growth increasing the immobile Bio-Region. Currently, TOUGHREACT does not consider the dynamic changes in the volume of immobile bio-region. The dynamic changes in porosity and volume will be implemented and explored in the future. Currently, we simply let the run stop at 7 days and then restart by increasing the immobile Bio-Region to 25% of the bulk porosity. The 14-day curve of 25% immobile region captures the observed data (Figure 5). Only one data point at (x = 0.0167) was off the curve, possibly because of other reasons (such as measurement errors). Overall the

multi-region model simulation matches better than the models of previous investigators (Doussan, 1997; Zysset et al., 1994). The simulated concentrations of dissolved organic carbon (DOC) and biomass obtained are presented in Figure 6. DOC decreases slowly here and is not a limiting factor for the bacterial growth. The growth is insignificantly slow until 7 days; then it accelerates dramatically.

The matches were adjusted with the interficial area A between Hydro- and Bio-Regions. The calibrated values are 38 m^2 per cubic bulk medium for the initial period, 75 m^2 for the late period. The better match and parameter calibration suggest that TOUGHREACT can not only be a useful interpretative tool for biogeochemical experiments, but also can produce insight into processes and parameters of microscopic diffusion and their interplay with biogeochemical reactions. It may provide a framework for understanding field-scale hydrobiogeochemical heterogeneities and upscaling parameters. Even though by adjusting bacterial growth rate parameters (specific growth rate and half-saturation constants) the 1-D porous medium model might reproduce the concentration profile, it is believed that the geometric- and process-based multi-region approach employed here could have predictive capability.

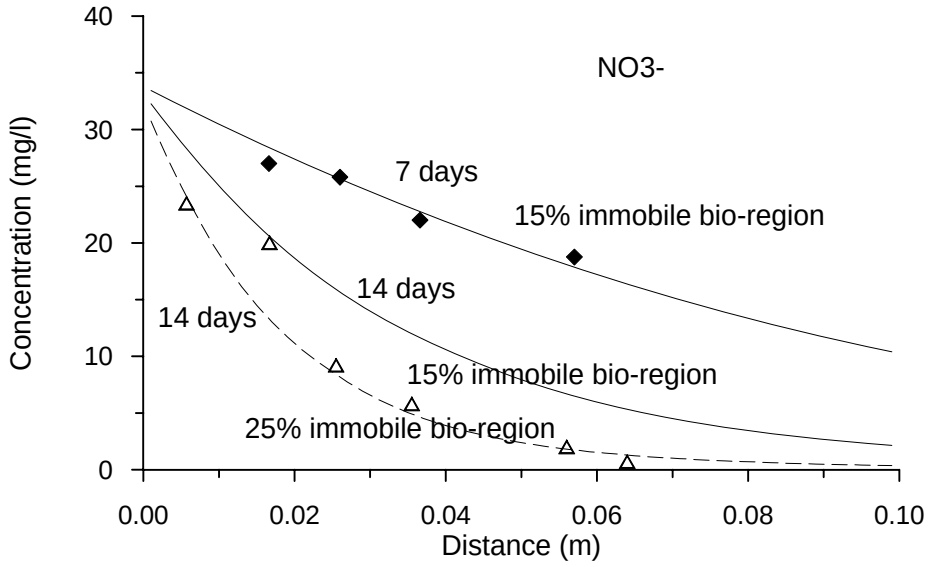

Figure 5. Nitrate concentrations obtained with the multi-region model after 7 and 14 days, together with measured data.

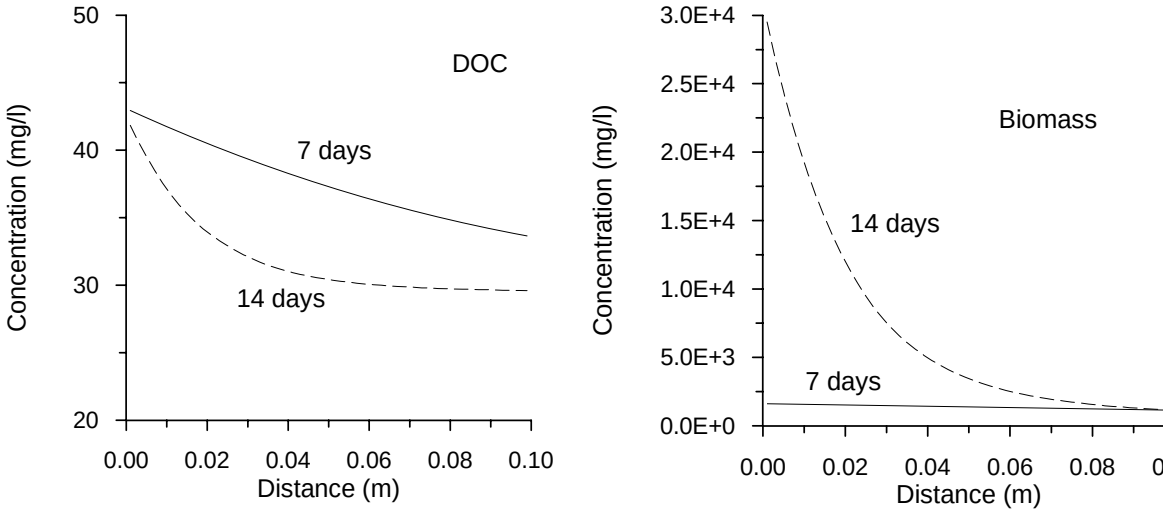

(a) DOC (b) Biomass

Figure 6. Concentrations of dissolved organic carbon (DOC) and biomass obtained with the multi-region model after 7 and 14 days.

5.4. Sulfate reduction

The evolution of sulfate in the Column 2 experiment of von Gunten and Zobrist (1993) was simulated together with that of oxygen and nitrate. Organic matter is successively oxidized by oxygen, nitrate, and sulfate. Denitrification is inhibited by oxygen, whereas sulfate reduction is inhibited by both oxygen and nitrate. A multi-region model was run using 25% of the bulk porosity (0.4) for the immobile Bio-Region throughout the simulation. The increased Bio-Region volume was attributed to (1) a longer simulation time (35 over 14 days) and (2) more electron acceptors (three over one). An interficial area of 75 m^2 per cubic meter bulk medium, calibrated from the simulation of 7 to 14 day of Column 1 was used for the simulation of Column 2. The two columns have different injection flow rates (1.83 m/day for Column 1, and 0.37 m/day for Column 2). All other physical parameters were assumed to be the same as Column 1, because the sediment material is the same in both columns. Simulated concentrations of sulfate captured the measured data well (Figure 7). According to von Gunten and Zobrist (1993), the spatial resolution of the experiments did not allow for clear separation of oxygen respiration from denitrification. Virtually complete nitrate reduction took place

within the first several centimeters of the flow distance. The simulation results are consistent with the nitrate observations.

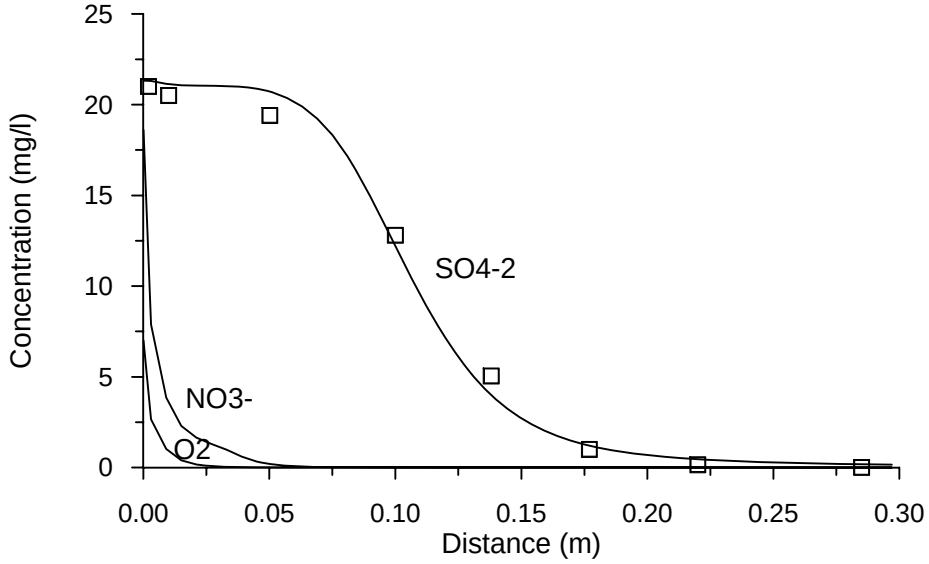

Figure 7. The simulated concentration profiles (lines) of sulfate, nitrate, and oxygen at steady-state (35 days), together with measured data of sulfate in column 2.

The simulated concentrations of dissolved organic carbon (DOC) and biomass (in the Bio-Region) obtained are presented in Figure 8. DOC profiles decreases over the distance due to biodegradation. Bacteria grow significantly close to the inlet owing to oxygen respiration and denitrification. Then a second growth peak occurs at about 0.05 m due to the start of sulfate reduction.

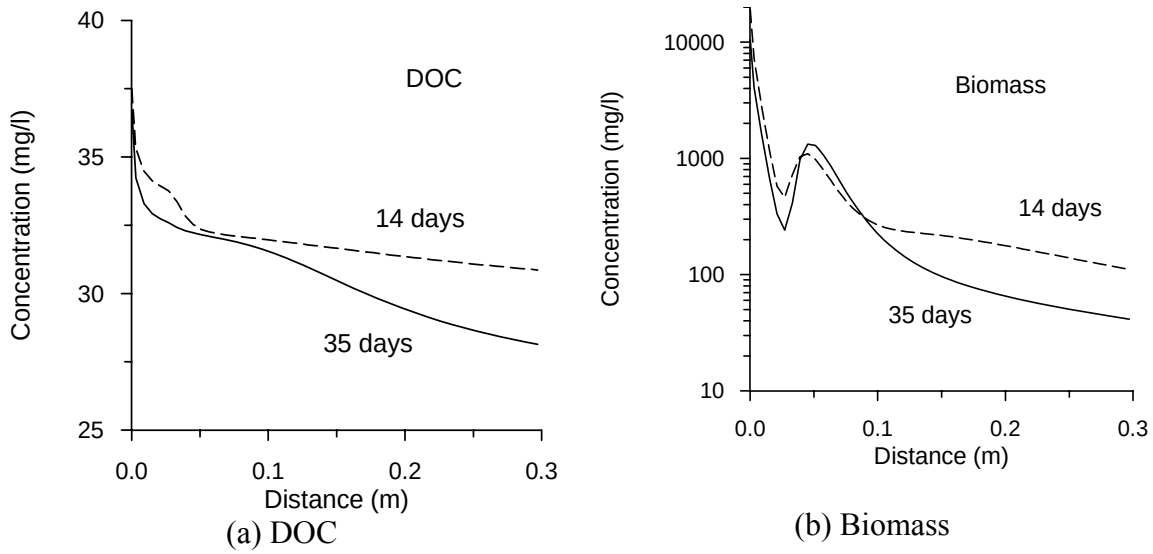

Figure 8. Concentrations of dissolved organic carbon (DOC) and biomass for Column 2.

5.5. Interacting with the Chem-Region

To illustrate the possible participation of minerals in the Chem-Region (solid particle), and the interplay between biodegradation and geochemical reactions, two reactive minerals gypsum and goethite were assumed to be initially present in the region. SO_4 dissolved from gypsum diffuses to the Bio-Region and then is reduced to HS. In the Chem-Region, Fe generated from goethite dissolution and HS diffused back from the Bio-Region may precipitate as pyrite. Ca from gypsum and HCO_3 from organic matter biodegradation may form calcite. The later two minerals were specified as potential secondary minerals. A simple rate law was used for mineral dissolution and precipitation:

$$r = kA\left[1 - \left(\frac{Q}{K}\right)\right] \tag{18}$$

where r is the kinetic rate (positive values indicate dissolution, and negative values precipitation), k is the rate constant (moles per unit mineral surface area and unit time), A is the specific reactive surface area per kg H_2O, K is the equilibrium constant for the

mineral-water reaction written for the destruction of one mole of mineral, and *Q* is the reaction quotient. The parameters used for the rate law Equation (18) are presented in Table 9. Rate constants for goethite and pyrite were increased by 5 orders of magnitude from the values in Palandri and Kharaka (2004), who compiled and fitted many of the experimental data reported by a large number of investigators. The rate increase was for explicitly accounting for bacterial catalysis. The dissolution-rate constants for gypsum and calcite were assigned to be two times those of goethite and pyrite. The assigned geochemical reaction rates could be comparable to sulfate bio-reduction. Note that a general multi-mechanism rate law was implemented in TOUGHREACT (Xu et al., 2006). It should also be mentioned that typically the abundant iron in sediments is present as Fe(III) and it inhibits sulfate reduction. This inhibition effects is not considered here. However, in the pH range of natural waters, Fe(III) is extremely insoluble and dissolved iron exists mainly as Fe(II) (von Gunten and Zobrist, 1993).

Table 9. List of parameters for calculating kinetic rate of dissolution and precipitation of minerals.

Mineral	*Chemical formula*	*Volume fraction (%)*	*Specific surface area (cm^2/g)*	*k ($mol/m^2/s$)*
Gypsum	$CaSO4 \bullet 2H_2O$	4	9.8	5.0×10^{-7}
Goethite	FeOOH	2	9.8	2.5×10^{-7}
Pyrite	FeS_2	0	9.8	2.5×10^{-7}
Calcite	$CaCO_3$	0	9.8	5.0×10^{-7}

The biogeochemical simulation of the multi-region model was based on sulfate reduction of Column 2, using 25% of the bulk porosity for the immobile Bio-Region and an interficial area of 75 m^2 per cubic meter medium. An increased initial biomass concentration of 60 mg/l was used to allow for significant biodegradation from the start. Initial concentrations for all other species are set equal to a very small value. Only DOC is assumed to be available in the injection water, with a concentration of 10 mg/l. The only electron acceptor SO_4 results from the leaching of the materials in the Chem-Region (gypsum dissolution).

Simulation results are presented in Figure 9 and 10. SO_4 concentrations increase along the distance (Figure 9a) because of gypsum dissolution (Figure 10b; Ca

concentrations take on the same pattern). Significant SO_4 concentration gradients occurs between Chem- and Bio-Regions because of (1) consumption by sulfate reduction in the Bio-Region and (2) larger d of Chem-Bio (3×10^{-5} over 2×10^{-5} m) and smaller τ (see Table 9). SO_4 concentration in the Bio-Region is slightly higher than that in the Hydro-Region. HS concentrations are higher in the Bio-Region due to sulfate reduction there (Figure 9b), but its concentrations are reduced in the Chem-Region resulting from the sink of pyrite precipitation (Figure 10d). HCO_3 concentrations increase (Figure 9c) and DOC decrease (Figure 9d) along the distance because of biodegradation. The difference of the latter two species among the three regions is very small.

Bacterial growth rates over the distance (Figure 10a) increase close to the inlet, because of the increase in SO_4 concentration, but later downstream decreases due to the low DOC concentrations. Biomass concentrations increase over time almost linearly. Returning to the Chem-Region, pyrite precipitation pattern is similar to goethite dissolution. The former volume is slightly larger than the latter because of the slightly larger mole volume (23.94 over 20.82 cm^3/mol). Calcite was not found in the simulation for the shorter column distance, but it could form along flow path if the distance was long enough, because the HCO_3 concentrations steadily increase (Figure 9c). Gypsum dissolution promotes bio-reduction of sulfate. Then the bio-generation of HS reacts with Fe from goethite dissolution, resulting in pyrite precipitation. Geochemical processes in the Chem-Region and micro-biological processes in the Bio-Region influence each other via micro-diffusion.

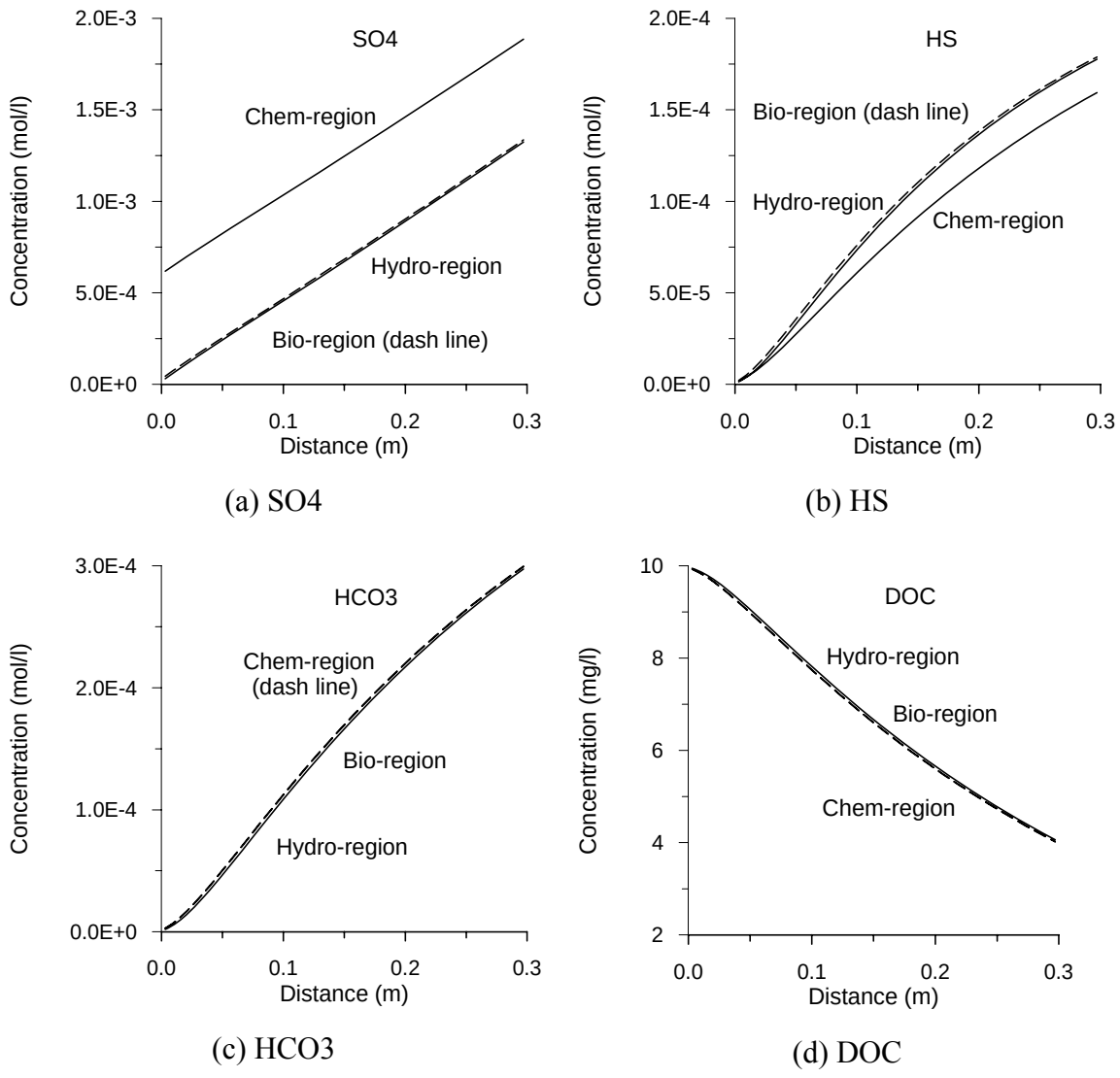

Figure 9. Concentrations of dissolved components at three regions after 13 days for the biogeochemical simulation.

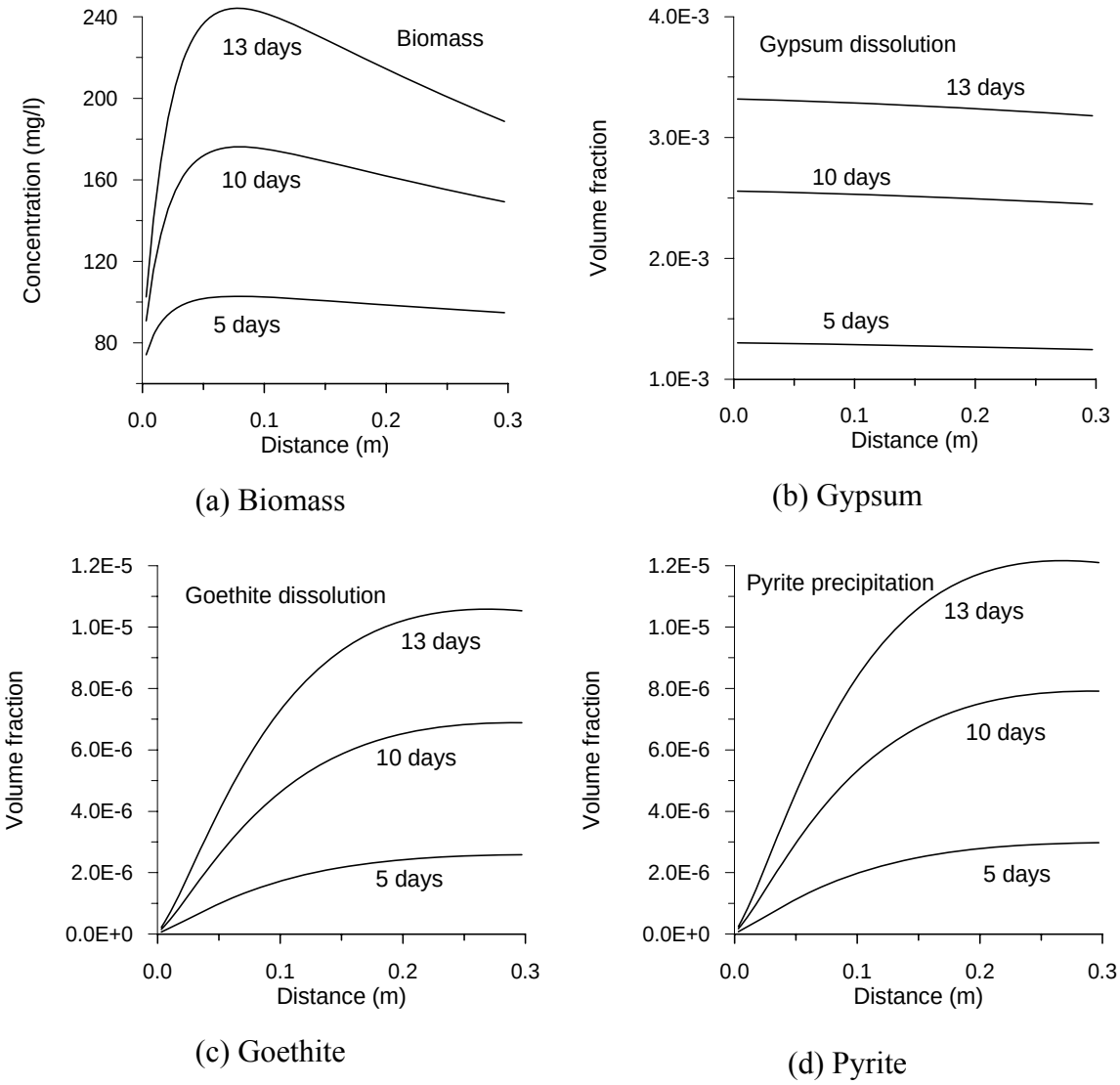

Figure 10. Biomass concentrations in the Bio-Region (a) and mineral dissolution and precipitation in the Chem-Region (b, c, and d) at different times.

6. Conclusions

Aqueous and sorption kinetics and microbiological processes have been incorporated into TOUGHREACT. This added capability was tested by 1-D reactive transport problem that involved kinetic biodegradation and sorption. Simulation results agree very well with those obtained by other simulators. The flexible space discretization, based on an integral finite difference approach, can use irregular gridding to model bio-

geologic structures. TOUGHREACT can deal directly with general multi-region (Hydro-Bio-Chem-region) and multiple interacting continua models for saturated and unsaturated porous and fractured media.

The applicability of this enhanced multi-region model for reactive transport of denitrification and sulfate reduction was validated by column experiments. The matches with measured nitrate and sulfate concentrations were adjusted with the interficial area between Hydro- and Bio-Regions. The values of 38 m^2 per cubic bulk medium for the initial period and 75 m^2 for the late period were calibrated. The better match and parameter calibration suggest that TOUGHREACT can not only be a useful interpretative tool for biogeochemical experiments, but also can produce insight into the processes and parameters of microscopic diffusion and their interplay with biogeochemical reactions. It may provide a framework for understanding field-scale hydrobiogeochemical heterogeneities and upscaling parameters, which should be explored in the future. Even though by adjusting bacterial growth rate parameters the 1-D porous medium model might reproduce the concentration profile, the geometric- and process-based multi-region approach employed here could provide greatly enhanced predictive capability. The interacting of an immobile "Bio-Region" with solid particles consisting initially of reactive-minerals gypsum and goethite, was modeled. Gypsum dissolution promotes bio-reduction of sulfate, after which the bio-generation of HS reacts with Fe from goethite dissolution, resulting in pyrite precipitation. It has been shown that geochemical processes in the "Chem-Region" and micro-biological processes in the "Bio-Region" influence each other via micro-diffusion.

The resulting biogeochemical-transport-simulation capabilities will be useful for many subsurface problems, including acidic mine drainage remediation, organic matter decomposition, oil and gas maturation, sulfite reduction in oil fields, and effective environmental remediation of groundwater contamination.

Acknowledgments. The author thanks Nicolas Spycher and Karsten Pruess for reviews of the manuscript and the constructive discussion. The author appreciates Guoxiang Zhang for providing the numerical data of Bio-CORE2D simulation. This work was first supported by the Director, Office of Science, Office of Basic Energy Sciences, of the U.S. Department of Energy, and later supported by the Laboratory Directed Research and Development Program (for the denitrification problem), under Contract No. DE-AC02-05CH11231 with Lawrence Berkeley National Laboratory. Support from an NSF-funded project is also acknowledged.

REFERENCES

Curtis, G.P., Comparison of approaches for simulating reactive solute transport involving organic degradation reactions by multiple terminal electron acceptors, Computer & Geoscience, Vol. 29, p. 319-329, 2003.

Doussan, C., G. Poitevin, E. Ledoux, M. Detay, River bank filtration: modelling of the changes in water chemistry with emphasis on nitrogen species, Journal of Contaminant Hydrology, 25 129-156, 1997.

Gwo, J. P., Jardine, P. M., Wilson, G. V., and Yeh, G. T., 1996, Using a multiregion model to study the effects of advective and diffusive mass transfer on local physical nonequilibrium and solute mobility in a structured soil: Water Resource Research, v. 32, p. 561-570.

Harvey, R.W., George, L.H., Smith, R.L. and Leblanc, D.R., 1989. Transport of microspheres and indigenous bacteria through a sandy aquifer: results of a natural and forced gradient tracer experiment. Environ. Sci.Technol., 23: 51-56.

Martin, G., 1985. Point sur l'6puration et le traitement des effluents, 2.2. Bact6riologie des milieux aquatiques. Lavoisier, Toulouse, 220 pp.

Narasimhan, T.N., Witherspoon, P.A., 1976. An integrated finite difference method for analyzing fluid flow in porous media, Water Resources Research, 12, 57–64.

Palandri, J., Kharaka, Y.K., 2004. A compilation of rate parameters of water-mineral interaction kinetics for application to geochemical modeling. US Geol. Surv. Open File Report 2004-1068, 64 pp.

Parkhurst, D.L., Appelo, C.A.J., User's Guide to PHREEQC (Version 2)—A computer program for speciation, batch-reaction, one-dimensional transport, and inverse geochemical calculations, USGS Water-Resources Investigations Report 99-4259, Denver, Colorado, 1999.

Pruess, K., and Narasimhan, T. N., 1985, A practical method for modeling fluid and heat flow in fractured porous media: Society of Petroleum Engineers Journal, v. 25, p. 14-26.

Pruess, K., Oldenburg, C., and Moridis, G., TOUGH2 user's guide, Version 2.0, Lawrence Berkeley Laboratory Report LBL-43134, Berkeley, California, 1999.

Simunek, J., Suares, D.L., 1994. Two-dimensional transport model for variably saturated porous media with major ion chemistry. Water Resource Research, 30, 1115-1133.

Sonnenthal E., A. Ito, N. Spycher, M. Yui, J. Apps, Y. Sugita, M. Conrad, and S. Kawakami, Approaches to modeling coupled thermal, hydrological, and chemical

processes in the Drift Scale Heater Test at Yucca Mountain. *International Journal of Rock Mechanics and Mining Sciences*, 42, 6987-719, 2005.

Spycher N.F., E.L. Sonnenthal, and J.A. Apps, Fluid flow and reactive transport around potential nuclear waste emplacement tunnels at Yucca Mountain, Nevada, *J. Contam. Hydrol.*, v. 62-63, p. 653-673, 2003.

Steefel, C. I., and K. T. B. MacQuarrie, Approaches to modeling of reactive transport in porous media, In Lichtner, P. C., Steefel, C. I., and Oelkers, E. H. (eds.), Reactive transport in porous media: Reviews in Mineralogy, Mineral Society of America, v. 34, p. 83-129, 1996.

Steefel, C.I., Incorporating Intra-Aqueous Kinetics into Reactive Transport Models, Presentation in Reactive Transport Workshop, Richland, Washington, 1997.

Tebes-Stevens, C., Valocchi, A.J., van Briesen, J.M., Rittmann, B.E., Multicomponent transport with coupled geochemical microbiological reactions: Model description and example simulations, Journal of Hydrology, 209, 8-26, 1998.

van Beelen, P. and Fleuren Kemila, K., 1989. Enumeration of anaerobic and oligotrophic bacteria in subsoils and sediments. J. Contam. Hydrol., 4:275 284.

von Gunten, U. and Zobrist, J., 1993. Biogeochemical changes in groundwater infiltration systems: column studies. Geochim. Cosmochim. Acta, 57: 3895-3906.

Wunderly, M. D., Blowes, D. W., Frind, E. O., and Ptacek C. J., 1996, Sulfide mineral oxidation and subsequent reactive transport of oxidation products in mine tailings impoundments: A numerical model: Water Resource Research, v. 32, p. 3173-3187.

Xu, T., Pruess, K., Brimhall, G., An improved equilibrium-kinetics speciation algorithm for redox reactions in variably saturated flow systems. Computers & Geosciences, 25(6), 655-666, 1999.

Xu, T., Pruess, K., Modeling multiphase non-isothermal fluid flow and reactive geochemical transport in variably saturated fractured rocks: 1. Methodology. American Journal of Science, 301, 16-33, 2001.

Xu, T., E.L. Sonnenthal, N. Spycher, and K. Pruess, TOUGHREACT user's guide: A simulation program for non-isothermal multiphase reactive geochemical transport in variable saturated geologic media, Lawrence Berkeley National Laboratory Report LBNL-55460, pp. 192, 2004.

Xu, T., E.L. Sonnenthal, N. Spycher, and K. Pruess, TOUGHREACT: A simulation program for non-isothermal multiphase reactive geochemical transport in variably saturated geologic media, Computer & Geoscience, Vol 32/2 pp 145-165, 2006.

Yeh, G.T., Tripathi, V.S., 1991. A model for simulating transport of reactive multispecies components: model development and demonstration. Water Resource Research, 27, 3075-3094.

Zhang, G., Non-isothermal hydrobiogeochemical models in porous media, PhD dissertation, University of La Corunia, Spain, 2001.

Zysset, A., Stauffer, E. and Dracos, T., 1994. Modelling of reactive groundwater transport governed by biodegradation. Water Resour. Res., 30: 2423-2434.